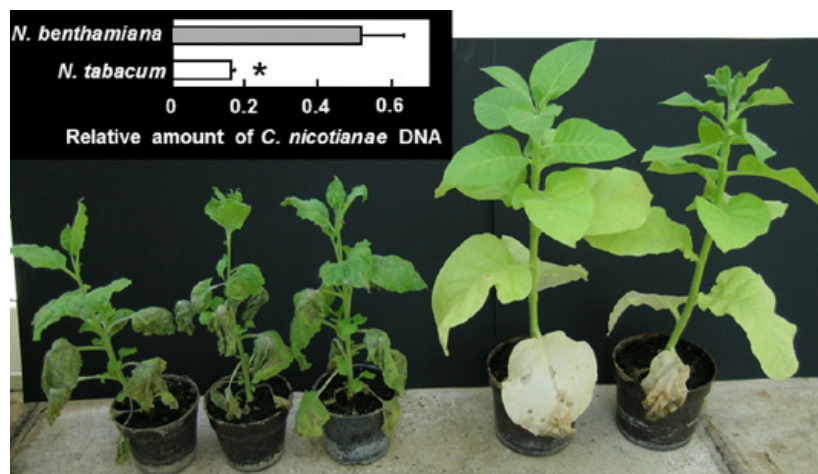
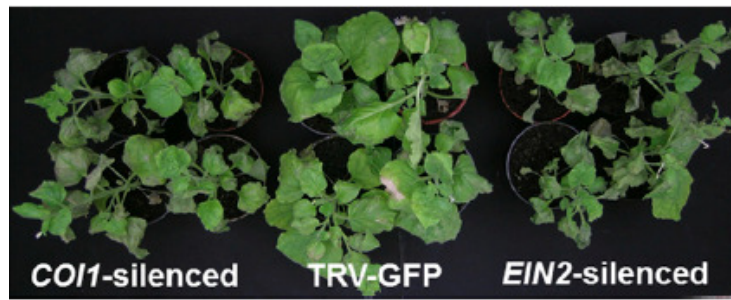


We described *Cercospora nicotianae* as a novel anamorphic ascomycete fungal pathogen of *Nicotiana benthamiana*, an important model plant in functional plant genomics. *N. benthamiana* is not only stunningly more susceptible to *C. nicotianae* than the conventional host of the fungus (*N. tabacum*) (**Figure 1**), but the two organisms together provide a useful new pathosystem for virus-induced gene silencing (VIGS). Silencing two crucial immune regulators of *N. benthamiana* (*COI1* and *EIN2*) led to a marked reduction in the resistance of the host to *C. nicotianae* (**Figure 2**). The relevance of this pathosystem is accentuated by the fact that *C. nicotianae* secretes a non-host specific toxin (cercosporin) in the infected plant tissues and cercosporin generates the formation of the reactive oxygen species (ROS) singlet oxygen when exposed to light making this pathosystem a convenient tool for studying singlet oxygen biology. The paper showing these results has been published in the Q1 journal *Phytopathology* (Fodor et al. 2018). In addition, an article presenting some results of this topic in Hungarian was released earlier (Tóth et al. 2015). An electroporation method for *Agrobacterium tumefaciens* was also developed within the frames of this part of the project which resulted in a methods paper published in the Springer journal *3 Biotech* (Kámán-Tóth et al. 2018).



**Fig. 1.** Symptoms of *Cercospora* leaf spot on 9-week-old *N. benthamiana* plants (3 plants on the left) and 12-week-old *N. tabacum* plants (2 plants on the right) 9 days after inoculation with the fungus. Plants were inoculated with a suspension of *C. nicotianae* conidia in a concentration of  $5 \times 10^4$  spores per milliliter. **Inset:** Relative amount of *C. nicotianae* to *N. tabacum* and *N. benthamiana* DNA in leaves 9 days after inoculation with the fungus. DNA levels were estimated by quantitative polymerase chain reaction specific for actin genes of *C. nicotianae*, *N. tabacum* and *N. benthamiana*. Bars represent mean  $\pm$  standard error of four biological and three technical replicates (each biological sample was composed as a pool of three plants). Total genomic DNA was extracted from 4 leaves (in positions 4 through 7) of plants for each species. Asterisk indicates statistically significant difference in relative amount of *C. nicotianae* DNA between *N. benthamiana* and *N. tabacum* plants calculated by Student's t-test ( $P \leq 0.01$ ).



**Fig. 2.** Suppression of *COI1* and *EIN2* transcript levels enhance symptoms caused by *C. nicotiana* on *N. benthamiana* plants (4 plants on the left and right, respectively). The GFP-silencing construct (TRV-GFP) was used as a control (4 plants in the middle). Plants were inoculated with a suspension of *C. nicotiana* conidia in a concentration of  $5 \times 10^4$  spores per milliliter. Picture was taken 7 days after inoculation.

### SOURCES AND ROLES OF AN EXTRACELLULAR OXIDATIVE BURST IN PATHOGEN-INDUCED CELL DEATH

An extracellular burst of reactive oxygen species (ROS) is a regular hallmark of pathogen attacks in plant tissues. The most intensively studied sources of this apoplastic ROS accumulation are the respiratory burst oxidase homolog (RBOH) NADPH oxidases localized in the cellular plasma membrane (Pogány et al. 2009).

There are, however, some important alternative sources of extracellular ROS, such as cell wall peroxidases and polyamine oxidases (Kärkönen and Kuchitsu 2015). Here we described roles of apoplastic cell wall peroxidase PRX33 and PRX34 in Arabidopsis plants challenged by the necrotrophic fungal pathogen *Alternaria brassicicola*. First the transcriptional activity of *PRX33* and *PRX34* genes was assessed by real-time RT PCR along with 5 Arabidopsis polyamine oxidase (*PAO*) isoforms after exposure to *A. brassicicola*. Transcript levels of *PRX33* and *PRX34* peroxidases were markedly raised by the fungal infection (**Figure 3**), whereas *PAO 1-5* genes were not induced (data not shown).

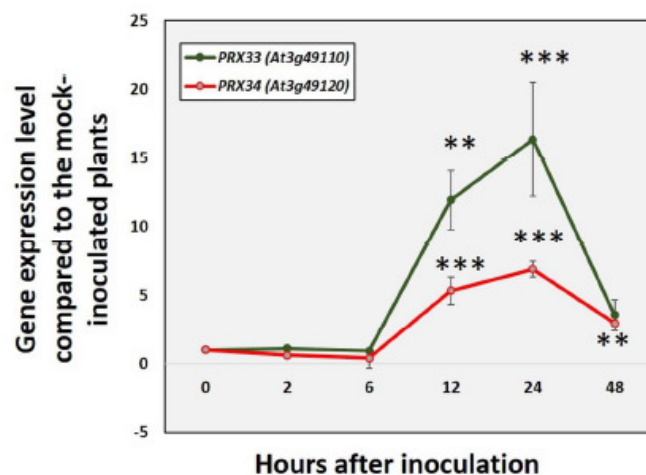


**Fig. 3.** *Alternaria brassicicola*-induced activation of *PRX33* and *PRX34* genes in wild type Arabidopsis plants. Five to 6 weeks old Arabidopsis plants (whole rosettes) were spray-inoculated with *A. brassicicola* conidium suspension used in a concentration of  $5 \times 10^5$  conidia in 1 mL distilled water. Data represent the mean of three independent biological samples with three technical replicates for each. Statistical analysis was performed using Student's t-test. Asterisks indicate statistically significant differences (\*\* $\alpha = 0.01$ , \*\*\* $\alpha = 0.001$ ).

Plants with reduced PRX33 and PRX34 transcript levels were acquired by ordering a *prx33* knock-down mutant (SALK\_062314C) from the Nottingham Arabidopsis Stock Centre and by generating a *PRX 33/PRX34* silencing VIGS construct (*TRV-PRX*), each validated for reduced *PRX33* and *PRX34* mRNA levels. When *prx33* and *TRV-PRX* plants were tested for their responses to *A. brassicicola* infection and ROS formation, they showed reduced necrotic symptoms, diminished fungal colonization and partly compromised ROS accumulation upon elicitation with the fungus (Figures 4, 5 and 6).

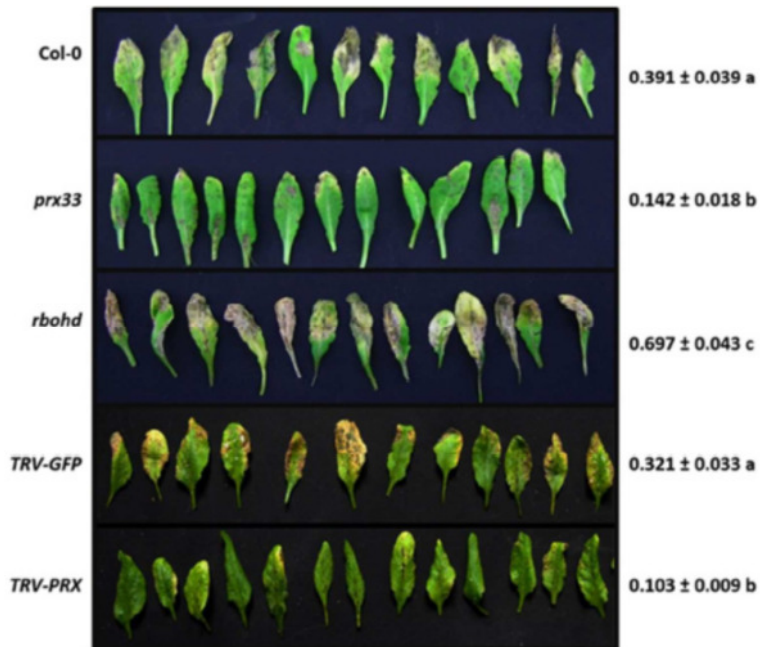


**Fig. 4.** Symptoms of *A. brassicicola* infection are suppressed in Arabidopsis plants with reduced *PRX33/PRX34* mRNA levels. Leaves of *A. brassicicola*-infected Col-0, *prx33* knock-down mutant, *rbohD* knock-out mutant, *TRV-GFP* and *TRV-PRX* plants are shown. Five to 6 weeks old Arabidopsis plants (whole rosettes) were spray-inoculated with *A. brassicicola* conidium suspension used in a concentration of  $5 \times 10^5$  conidia in 1 mL distilled water. Detached leaves in middle positions (5.-8. leaf levels) were evaluated. Results are presented as chlorotic and necrotic leaf area compared to the total surface of leaf blades analyzed by ImageJ (1 is equal to 100% leaf surface) and represent means of two experiments ( $n=30$  for each genotype/treatment)  $\pm$  SE. Different letters indicate statistically significant differences between genotypes/treatments using Tukey's posthoc test. Increased symptoms of *A. brassicicola* on leaves of the *rbohD* mutant are included as a reference.

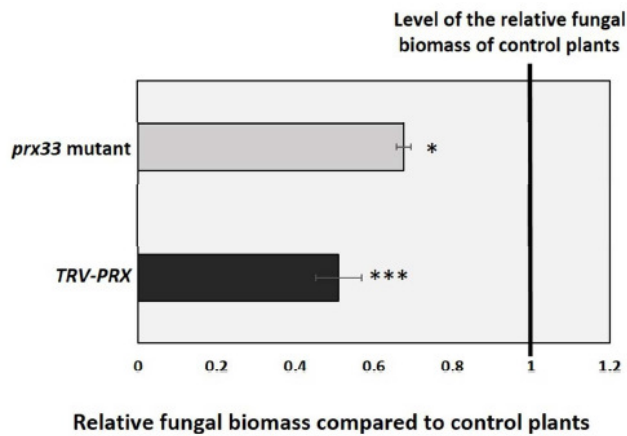


**Fig. 5.** *A. brassicicola* biomass in *prx33* T-DNA insertion line and in gene-silenced (*TRV-PRX*) plants. Five to 6 weeks old *Arabidopsis* plants (whole rosettes) were spray-inoculated with *A. brassicicola* conidium suspension used in a concentration of  $5 \times 10^5$  conidia in 1 mL distilled water. The results show the average of two experiments each comprising three biological samples (each sample composed as a pool of 3 *Arabidopsis* rosettes) analyzed in three technical replicates. Statistical analysis was performed using Student's t-test.

Asterisks indicate statistically significant differences between *PRX* knock-down *Arabidopsis* plants (*prx33*, *TRV-PRX*) and their controls (Col-0, *TRV-GFP*) 10 days after inoculation with *A. brassicicola* (\* $\alpha = 0.05$ , \*\*\* $\alpha=0.001$ ).

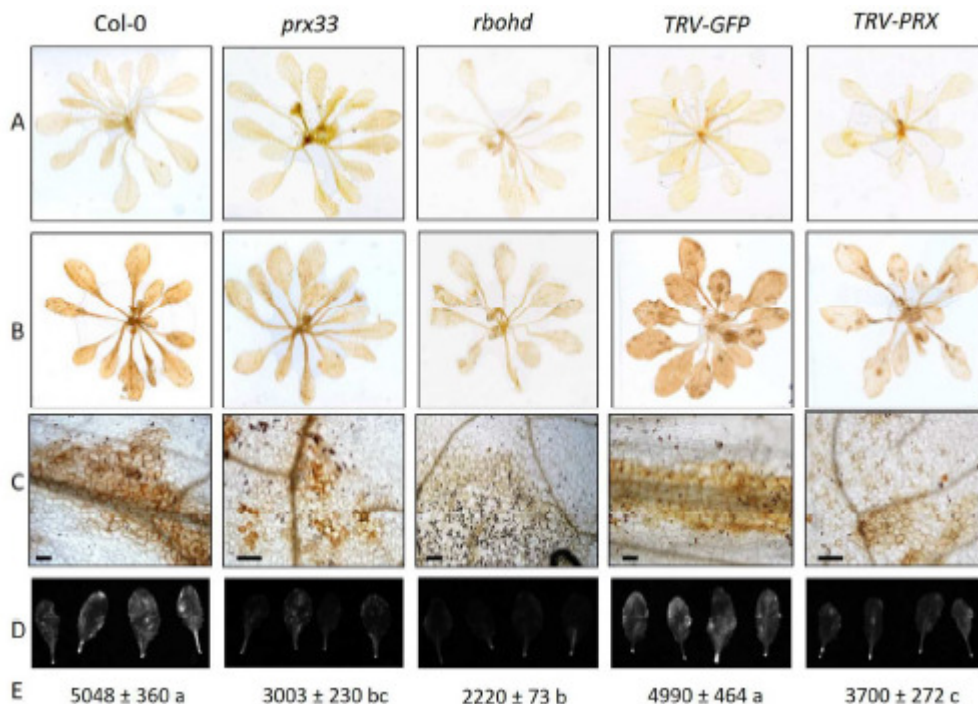


**Fig. 6.**  $H_2O_2$  production in *Arabidopsis* plants with reduced cell wall peroxidase or NADPH oxidase activity. The accumulation of  $H_2O_2$  was detected in wild-type (Col-0), *prx33* and *rbohD* T-DNA insertion lines and in *TRV-GFP* and *TRV-PRX* gene-silenced *Arabidopsis* plants by 3,3'-diaminobenzidine (DAB) (A-C) and 2',7'-dichlorofluorescein diacetate (DCFH-DA) staining methods (D, E). Five to 6 weeks old *Arabidopsis* plants (whole rosettes) were spray-inoculated with *A. brassicicola* conidium suspension used in a concentration of  $5 \times 10^5$  conidia in 1 mL distilled water. The stainings were carried out with mock-inoculated (A), and *Alternaria brassicicola*-infected plants (2 days after inoculation) (B-E). Bars = 50  $\mu$ m. The intensity of the fluorescence signal emitted by DCFH-DA-stained leaves (D) was quantified under UV light using an Alphascreen Mini gel documentation system (E). Results are presented as an average pixel fluorescence intensity and represent means of two experiments ( $n=30$  leaves in the middle position for each genotype/treatment)  $\pm$  SE. Statistical analysis was performed using one-way ANOVA and Tukey's posthoc test. Different letters indicate statistically significant results. *prx33* and *TRV-PRX* plants accumulate less hydrogen peroxide as compared to the corresponding control plants. Microscopic observation of patterns of hydrogen peroxide accumulation reveals that *prx33* and *TRV-PRX* plants show apoplastic  $H_2O_2$  accumulation in a reduced number of cells in comparison with the corresponding control plants after inoculation with *A. brassicicola*. Leaves of the *rbohD* knock-out line lacking apoplastic  $H_2O_2$  accumulation after *A. brassicicola* infection are shown as a reference. Decreased  $H_2O_2$  production in *rbohD* plants was also confirmed by the DCFH-DA staining method. The mean level of base fluorescence for mock-inoculated Col-0 plants was  $1240 \pm 34$ .

We concluded from these results that PRX33/PRX34-derived ROS most likely function in *Arabidopsis* as susceptibility factors when plants are challenged by the necrotrophic fungal pathogen *Alternaria brassicicola*.

Moreover, PRX33/PRX34 apoplastic peroxidases may also have a role in the spread of intercellular ROS signaling initiated by the NADPH oxidase RBOHD, as it was indicated by our microscopic results (**Figure 6**). An age-dependent transcript distribution of ROS-producing peroxidase and NADPH oxidase enzymes and some potential new components of the RBOHD, PRX33 and PRX34 signaling networks were also revealed (data not shown). The manuscript that includes this set of results is currently under the second round of reviewing at the D1 journal of Wiley Molecular Plant Pathology (Kámán-Tóth et al. 2018).

Another paper revealing the connection between cold hardening of cereals (wheat and barley), their oxidative stress tolerance and resistance to the necrotrophic fungal pathogen *Pyrenophora teres* f. *teres* has been also published (Pogány et al. 2016). Moreover, a review paper on the molecular aspects of pathogenesis caused by *Alternaria* fungi was published in Hungarian (Kámán-Tóth et al. 2016).

## RESULTS WITH A PREVIOUSLY UNCHARACTERIZED PROTEOLYTIC FACTOR IN ARABIDOPSIS

In a search for new proteolytic regulators of Arabidopsis immunity a set of nearly 100 Arabidopsis mutants impaired in the function of various genes encoding proteins with proteolytic activity was screened.

One mutant carrying an insertion in the 5th exon of a gene (*At4g10540*; *AtSbt3.8*) encoding a subtilisin-like serine protease (subtilase) was selected on the basis of its altered host responses to Arabidopsis pathogens. This mutant was markedly more susceptible to the necrotrophic fungus *Alternaria brassicicola* and to the hemibiotrophic bacterial pathogen *P. syringae* pv. *tomato* but was more resistant to the biotrophic powdery mildew fungus (*Golovinomyces orontii*) (**Figures 7, 8 and 9**).

These pathological results were also confirmed by developing a virus-induced gene silencing construct specifically designed to silence mRNA level of the same Arabidopsis subtilase gene *AtSbt3.8* (**Figure 10**).

The effect of *At4g10540* gene activity on the transcriptomic response of diseased plants was assessed by performing cDNA microarray analyses from pathogen-infected wild type and mutant Arabidopsis samples. Six hours after inoculation mRNA expression of over 500 genes were significantly different between the mutant and the wild type Arabidopsis lines. Transcription of genes in the jasmonic acid signalling pathway are strikingly affected by the mutation in *At4g10540* locus. Our microarray data were validated by real-time RT PCR (**Figures 11 and 12**).

Expression of the gene *At4g10540* by RT-PCR and real-time RT PCR in mock- and *Alternaria*-inoculated plants revealed that the gene is transcribed at an extremely low level and is not substantially up-regulated even after pathogen treatment. By using roots of Arabidopsis plants grown in hydroponic culture, however, we were able to synthesise *At4g10540* cDNA that was sequenced, confirming mRNA expression of the gene. The cDNA got transferred into pGEM-T Easy vector and was used for further downstream recombinant DNA approaches.



In order to find out the intracellular localization of this particular Arabidopsis proteolytic enzyme, recombinant GFP fusion constructs have been made (still in a pGEM-T Easy vector system) transformed into *A. tumefaciens* cells and transiently expressed in *N. benthamiana* leaves. Samples were observed by confocal laser scanning microscope (CLSM). Intracellular localization of the AT4G10540 subtilisin-like serine protease (SBT3.8) has been linked to the cellular cytoplasm. Prior to CLSM detection shortened GFP fusion constructs have been prepared to avoid enzymatic removal of the GFP reporter tag along with a suspected C-terminal regulatory domain (**Figure 13**).

In 2009 the 3D structure of a tomato subtilase protein was described using X-ray crystallography (Ottmann et al. 2009). This information enabled us to generate a decent model on the structure of the translated protein encoded by our subtilase locus using I-TASSER and RasMol software packages. This bioinformatic analysis also included a prediction on the location of the catalytic triad of this protease (**Figure 14**).

A manuscript presenting these discoveries on the cellular functions of Arabidopsis ATSBT3.8 as a regulator of plant immunity to microbial pathogens is in preparation and two conference proceedings were previously released in Hungarian (Nagy et al. 2013, Dankó et al. 2017).

A review paper on regulatory non-proteasomal proteolysis in Arabidopsis has been published in the Q1 journal International Journal of Molecular Sciences (Pogány et al. 2015).

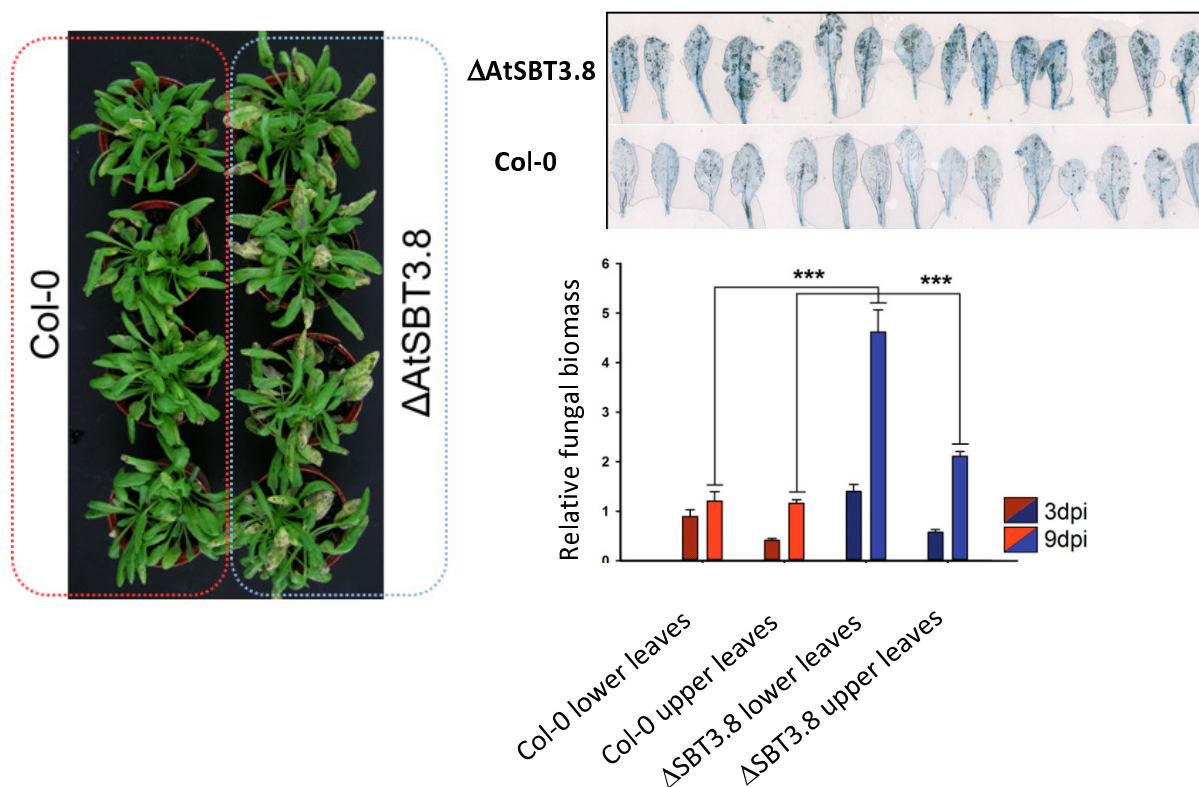


**Fig. 7.** The *sbt3.8* mutant Arabidopsis line ( $\Delta$ AtSBT3.8) is markedly more susceptible to the necrotrophic fungus *A. brassicicola* than the wild type (Col-0). Symptoms and PCR-based fungal biomass assessment were performed 9 days after inoculation with the fungus.

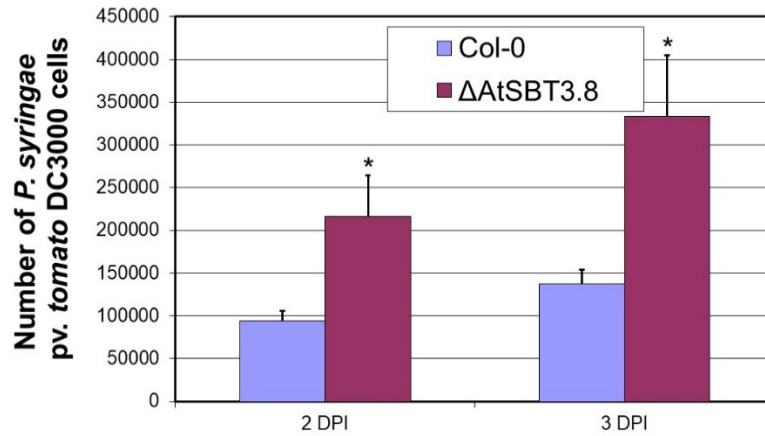


**Fig. 8.** The hemibiotrophic bacterial pathogen *P. syringae* pv. *tomato* strain DC3000 colonizes leaves of the *sbt3.8* mutant Arabidopsis line ( $\Delta$ AtSBT3.8) more efficiently than those of the wild type (Col-0). Number of bacterial cells were evaluated 2 and 3 days after inoculation.

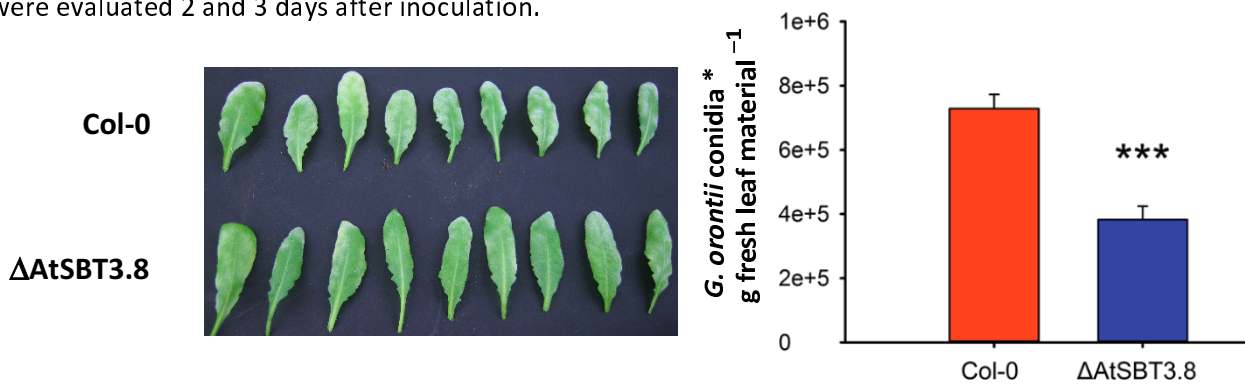


**Fig. 9.** The *sbt3.8* mutant Arabidopsis line ( $\Delta$ AtSBT3.8) is less susceptible to the biotrophic powdery mildew fungus *Golovinomyces orontii* than the wild type (Col-0). Fungal conidium formation on the two genotypes was evaluated 12 days after inoculation.

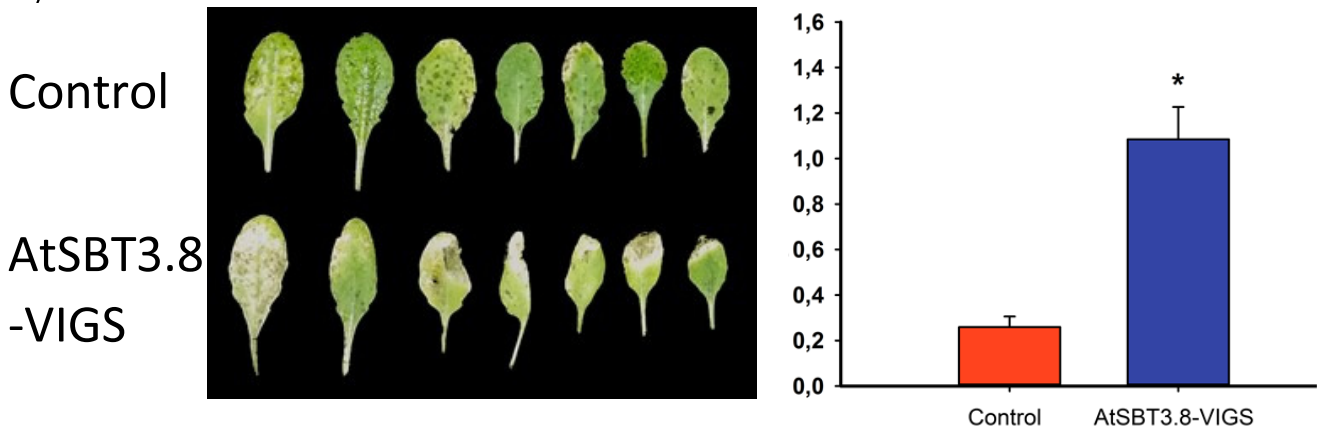


**Fig. 10.** Post-transcriptional gene silencing of *AtSbt3.8* by using a TRV-VIGS construct substantially increases susceptibility of Arabidopsis to the necrotrophic fungus *A. brassicicola*.

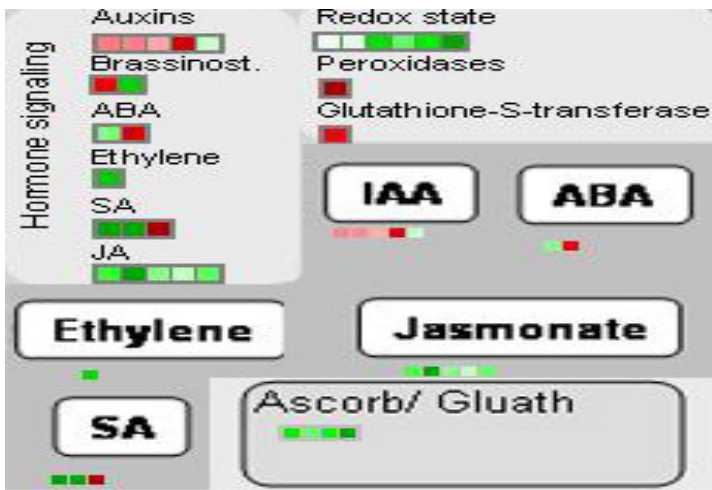


**Fig. 11.** Gene expression analysis of *P. syringae* pv. *tomato*-infected *sbt3.8* Arabidopsis plants 6 hours after inoculation with the pathogen. Hormone signaling (particularly jasmonate and auxin) is most strikingly affected as a result of ATSBT3.8 impairment.

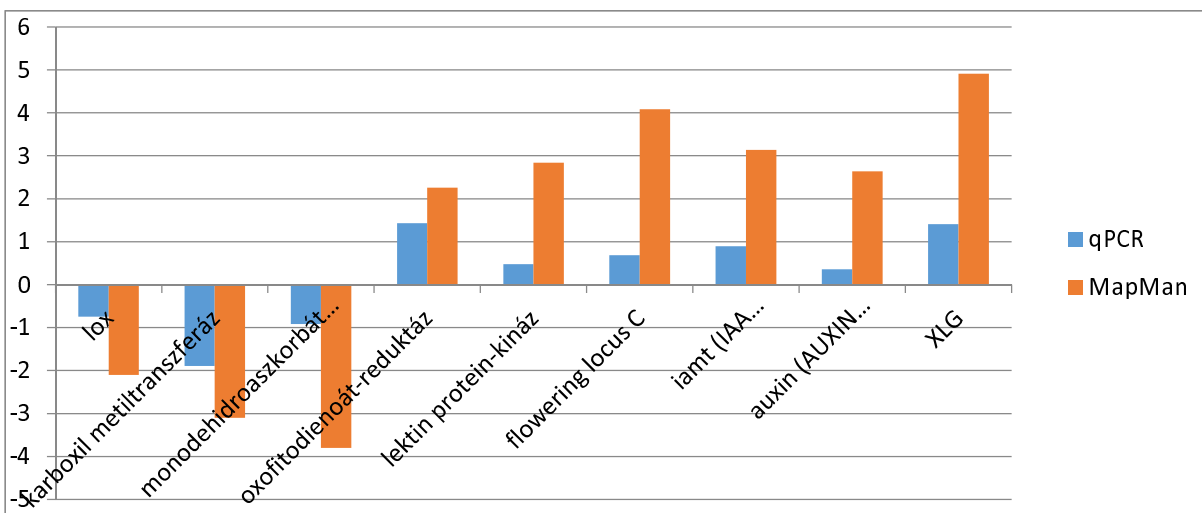


**Fig. 12.** Real-time RT PCR (qPCR) validation of microarray results.

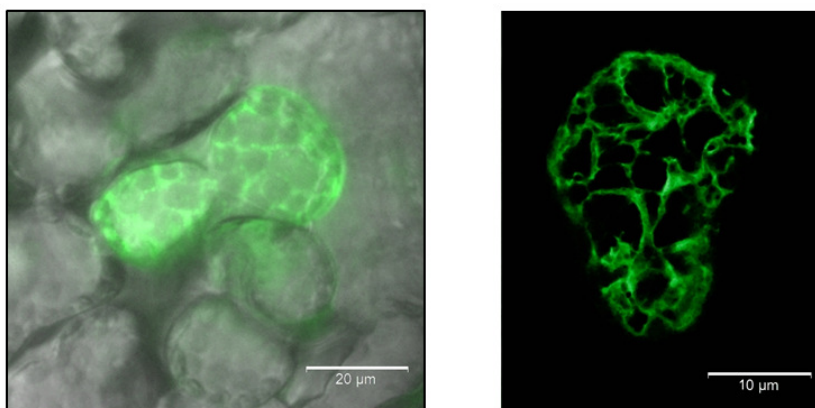


**Fig. 13.** Confocal laser scanning microscopy images of *N. benthamiana* cells transiently expressing a shortened *AtSbt3.8-GFP* fusion construct. Subcellular localization of the ATSBT3.8 subtilisin-like serine protease is linked to the cellular cytoplasm.



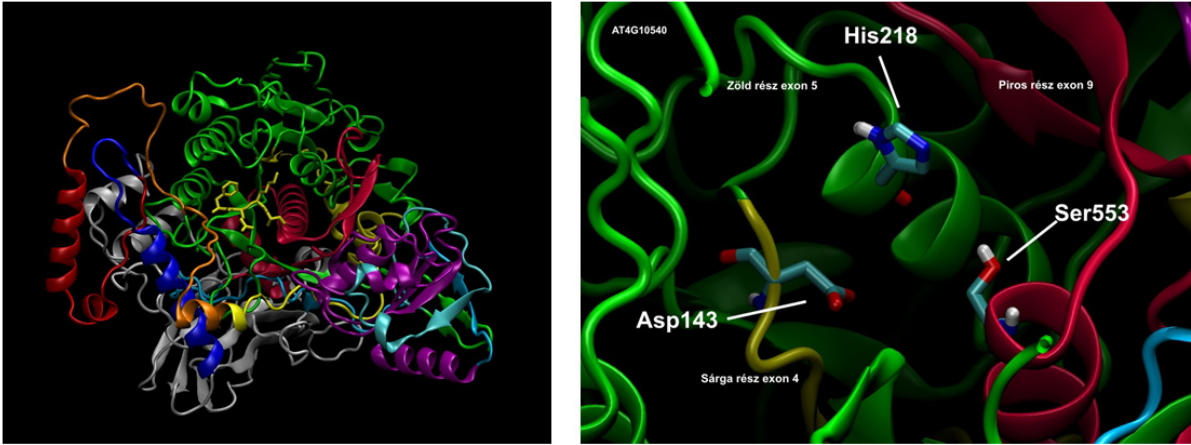


**Fig. 14.** The three-dimensional structure of ATSBT3.8 subtilase protein generated with I-TASSER software. Three critical amino acids (Asp143, His218 and Ser553) forming the catalytic triad of the protein are encoded in 3 different exons.

## RESULTS ON THE CONTRIBUTION OF CHLOROPLASTIC ROS FORMATION TO PATHOGEN-INDUCED CELL DEATH AND THE CELLULAR REDOX STATUS OF PLANTS

The chloroplasts and the photosynthetic activity of plant cells have been considered as pivotal components of cellular redox homeostasis. Their roles in the initiation of pathogen-induced cell death have also been implicated. In a straightforward set of experiments we inhibited the photosynthetic activity of *N. benthamiana* leaves by VIGS technology targeting phytoene desaturase (*PDS*) transcripts, a key enzyme in carotenoid (and chlorophyll) biosynthesis. Silencing of *PDS* in *N. benthamiana* results in remarkable, white, chlorophyll-deficient leaves. The experiments were performed with GFP (Green Fluorescent Protein)-expressing *N. benthamiana* plants and a marker GFP-silencing construct (TRV2-GFP) was used for control plants with normal photosynthesis (labelled here as *GFP*).

*PDS*-silenced and regular (green) plants with normal photosynthesis were inoculated with a model viral pathogen of tobacco, tobacco necrosis virus (TNV) causing necrotic lesions on inoculated leaves without systemic spread of the virus. Necrotic symptoms of the viral infection were drastically reduced in *PDS*-silenced tissues, both the density and diameter of necrotic lesions were suppressed in the white, chlorophyll-deficient leaves (**Figure 15**). Viral replication was also suppressed in *PDS*-silenced *N. benthamiana* tissues (**Figure 16**).

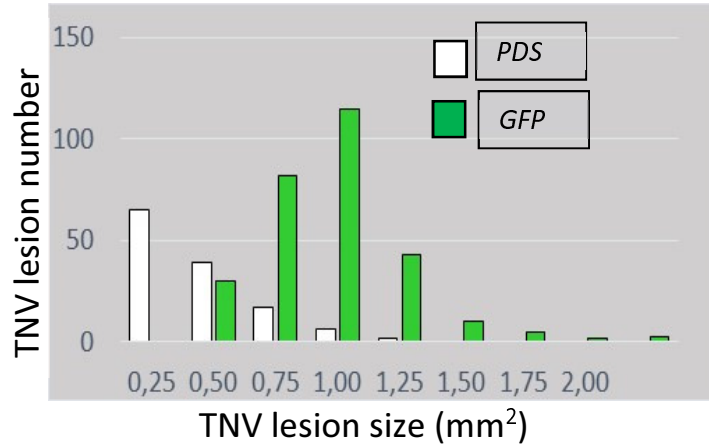


**Fig. 15.** PDS-silenced *N. benthamiana* plants (*PDS*) with inhibited photosynthesis show reduced necrotic symptoms after inoculation with TNV (3 dpi) in comparison with control (*GFP*-silenced) plants.

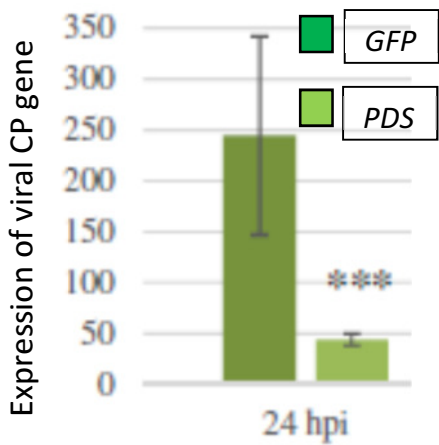


**Fig. 16.** Detection of TNV coat protein gene expression by qRT-PCR at 24 hpi revealed that replication of the virus is also suppressed in *PDS*-silenced *N. benthamiana* tissues.

It was also confirmed that the TNV-induced oxidative burst is abolished in the *PDS*-silenced tissues, whereas the control (green) tissues exhibit marked hydrogen peroxide accumulation 3 days after inoculation with the virus (**Figure 17**).

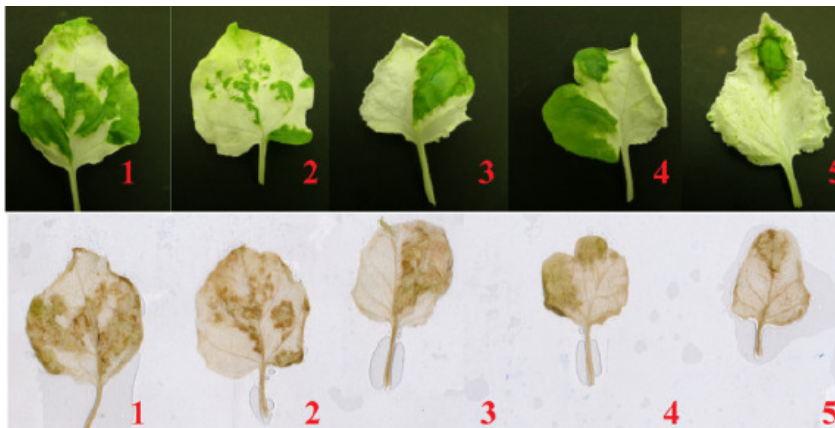


**Fig. 17.** Detection of hydrogen peroxide by 3,3'-diaminobenzidine (DAB) staining in *N. benthamiana* leaves with *PDS*-silenced (white) and non-silenced (green) sections 3 days after inoculation with TNV. Brown precipitate indicating ROS accumulation is limited to the green sections.

The redox homeostasis of *PDS*-silenced and control tobacco tissues was monitored by spectrophotometric antioxidant enzyme assays and real-time RT PCR detection of mRNA levels encoding proteins with antioxidant enzyme activity. *PDS*-silenced tissues showed pronounced alterations in their antioxidant status both before and after inoculation with TNV. Their catalase activity, for instance, was strongly reduced in comparison with control (photosynthesizing) tissues, supposedly as a result of transcriptional and posttranscriptional regulation (**Figure 18**).

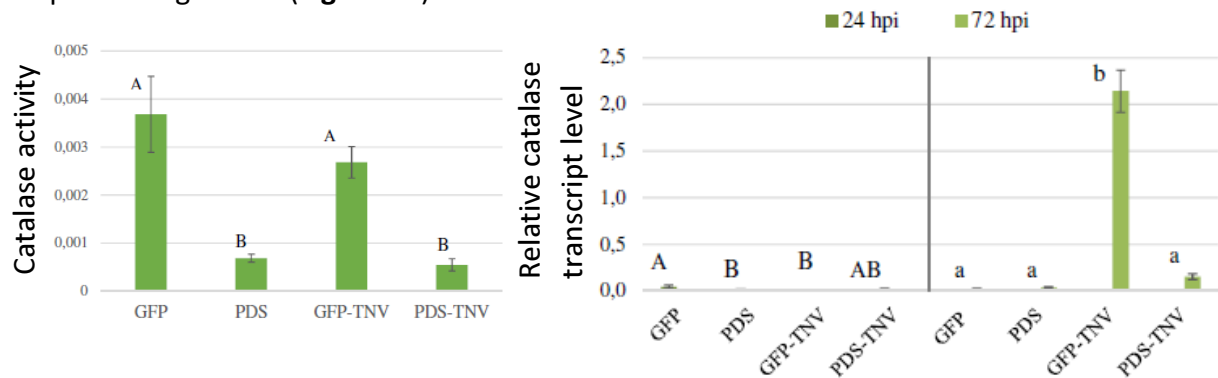


**Fig. 18.** Catalase activity (72 hpi) and catalase transcript levels (24 and 72 hpi) in *PDS*-silenced (PDS) and control (GFP) *N. benthamiana* tissues with or without TNV infection. Catalase activity is reduced in *PDS*-silenced tissues.

Transcriptional responses for the cell death regulator (and ROS producer), plasma membrane-localized NADPH oxidase *N. benthamiana* RBOH protein were also affected by *PDS*-silencing (**Figure 19**).

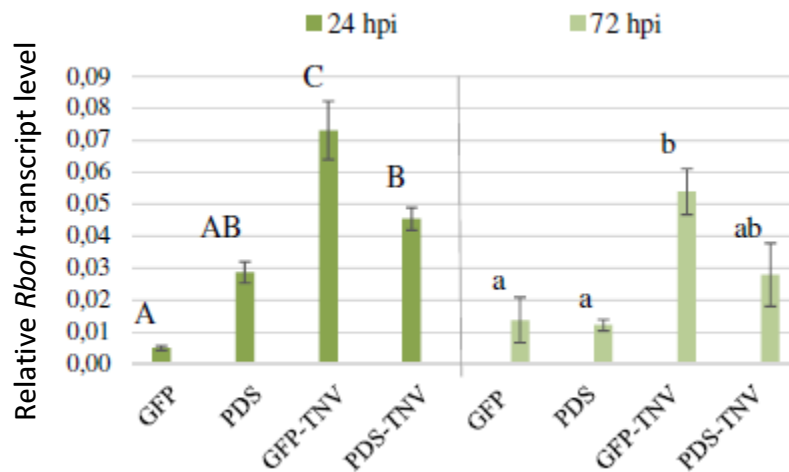


**Fig. 19.** Transcript abundance of the *N. benthamiana* cell death regulator Respiratory burst oxidase homologue (*Rboh*) in *PDS*-silenced (PDS) and control (GFP) tissues with or without TNV infection.

A manuscript presenting the contribution of chloroplast-derived ROS to cellular redox homeostasis of plants and pathogen-induced cell death is currently in preparation.

Additionally, three articles on the molecular biology of phage-phytobacterium interaction and the transcriptomics of plants infected with plant pathogenic bacteria were published within the frames of the project (Kolozsváriné-Nagy et al. 2015, Bozsó et al. 2016, Schwarczinger et al. 2017).

## REFERENCES

Bozsó Z, Ott PG, Kámán-Tóth E, Bognár GF, Pogány M and Szatmári Á (2016): Overlapping yet response-specific transcriptome alterations characterize nature of tobacco-*Pseudomonas syringae* interactions. *Front. Plant Sci.* 7, 251.

Dankó T, Kámán-Tóth E, Vági P, Gellért Á, Bozsó Z és Pogány M (2017): Az Arabidopsis AT4g10540 szubtiláz befolyásolja a növény kórokozókkal szembeni válaszát. In: 63. Növényvédelmi Tudományos Napok, 2017. február 21-22., Budapest Összefoglaló 91.

Fodor J, Kámán-Tóth E, Dankó T, Schwarczinger I, Bozsó Z and Pogány M (2017): Description of the *Nicotiana benthamiana-Cercospora nicotianae* pathosystem. *Phytopathol.* 108, 149-155.

Kámán-Tóth E, Palkovics L és Pogány M (2016): *Alternaria* fajok által okozott kórfolyamatok élettana és molekuláris biológiája növényekben. *Növényvédelem* 52, 557-566.

Kámán-Tóth E, Pogány M, Dankó T, Szatmári Á and Bozsó Z. (2018): A simplified and efficient *Agrobacterium tumefaciens* electroporation method. *3 Biotech* 8, 148.

Kámán-Tóth E, Dankó T, Gullner G, Bozsó Z, Palkovics L and Pogány M (2018): Contribution of cell wall peroxidase- and NADPH oxidase -derived reactive oxygen species to *Alternaria brassicicola*-induced oxidative burst in Arabidopsis. *Mol. Plant Pathol.* *Submitted*

Kärkönen, A. and Kuchitsu, K. (2015): Reactive oxygen species in cell wall metabolism and development in plants. *Phytochem.* 112, 22-32.

Kolozsváriné-Nagy J, Schwarczinger I, Künstler A, Pogány M and Király L (2015): Penetration and translocation of *Erwinia amylovora*-specific bacteriophages in apple - a possibility of enhanced control of fire blight. *Eur. J. Plant Pathol.* 142, 815-827.

Ottmann C, Rose R, Huttenlocher F, Cedzich A, Hauske P, Kaiser M, Huber R and Schaller A (2009): Structural basis for Ca<sup>2+</sup>-independence and activation by homodimerization of tomato subtilase 3. *Proc. Natl. Acad. Sci.* 106, 17223–17228.

Nagy VA, Pogány M, Bozsó Z és Tóth E (2013): Fehérjelebontó faktorok szerepének vizsgálata Arabidopsis thaliana kórokozókkal szembeni rezisztenciaválaszában. In: II. ATK Tudományos Nap, Velünk Élő Tudomány, 2013. november 8., Martonvásár, pp. 237-240.

Pogány M, Harrach B, Bozsó Z, Künstler A, Janda T, von Rad U, Vida Gy and Veisz O (2016): Cold hardening protects cereals from oxidative stress and necrotrophic fungal pathogenesis. *Open Life Sci.* 11, 78-85.

Pogány M, Dankó T, Kámán-Tóth E, Schwarczinger I and Bozsó Z (2015): Regulatory proteolysis in *Arabidopsis*-pathogen interactions. *Int. J. Mol. Sci.* 16, 23177-23194.

Pogány M, von Rad U, Grün S, Dongó A, Pintye A, Simoneau P, Bahnweg G, Kiss L, Barna B and Durner J. (2009): Dual roles of reactive oxygen species and NADPH oxidase RBOHD in an *Arabidopsis*-*Alternaria* pathosystem. *Plant Physiol.* 151, 1459-1475.

Schwarczinger I, Nagy JK, Künstler A, Szabó L, Geider K, Király L and Pogány M (2017): Characterization of Myoviridae and Podoviridae family bacteriophages of *Erwinia amylovora* from Hungary-potential of application in biological control of fire blight. *Eur. J. Plant Pathol.* 149, 639-652.

Tóth E, Czuppon B, Fodor J, Bozsó Z és Pogány M (2015) Egy molekuláris növénykórtani vizsgálatok céljára javasolható növény-gomba kölcsönhatás. *Növényvédelem* 51, 309-316.